Tobias Schripp, Tobias Grein, Julia Zinsmeister, Patrick Oßwald, Markus Köhler, Franziska Müller-Langer[1], Stephanie Hauschild[1], Christian Marquardt[2], Sebastian Scheuermann[2], Alexander Zschocke[3], and Dietmar Posselt[4], Technical Application of a Ternary Alternative Jet Fuel Blend – Chemical Characterization and Impact on Jet Engine Particle Emission, Fuel, 288 (2021) 119606.

[1] Deutsches Biomasseforschungszentrum (DBFZ), Biorefineries, Leipzig, Germany
[2] Wehrwissenschaftliches Institut für Werk- und Betriebsstoffe (WIWeB), Erding, Germany
[3] Deutsche Lufthansa AG, Köln, Germany
[4] Aviation Fuel Projects Consulting, Prien am Chiemsee, Germany

The original publication is available at
https://www.sciencedirect.com/science/article/abs/pii/S0016236120326028

https://doi.org/10.1016/j.fuel.2020.119606

Technical Application of a Ternary Alternative Jet Fuel Blend – Chemical Characterization and Impact on Jet Engine Particle Emission

Tobias Schripp[1*)], Tobias Grein[1)], Julia Zinsmeister[1)], Patrick Oßwald[1)], Markus Köhler[1)], Franziska Müller-Langer[2)], Stephanie Hauschild[2)], Christian Marquardt[3)], Sebastian Scheuermann[3)], Alexander Zschocke[4),*] and Dietmar Posselt[5)]

[1)] German Aerospace Center (DLR), Institute of Combustion Technology, Stuttgart, Germany
[2)] Deutsches Biomasseforschungszentrum (DBFZ), Biorefineries, Leipzig, Germany
[3)] Wehrwissenschaftliches Institut für Werk- und Betriebsstoffe (WIWeB), Erding, Germany
[4)] Deutsche Lufthansa AG, Köln, Germany
[5)] Aviation Fuel Projects Consulting, Prien am Chiemsee, Germany
* Current affiliation: Centre of Competence for Climate, Environment and Noise Protection in Aviation, Frankfurt am Main, Germany

Keywords: HEFA, alcohol-to-jet, soot, storage stability

Abstract

The use of alternative fuels is an essential element in future aviation. There are currently different approaches with regard to fuel production processes and feedstock materials. This requires flexible handling of available fuel quantities. The production of fuel mixtures (blends) is inevitable for an effective usage of commercially available fuel components. Within the framework of the project DEMO-SPK approx. 600 t of a ternary mixture (multiblend) of alternative jet fuels was produced and used in a real airport infrastructure at the airport Leipzig/Halle. Production and application were accompanied with extensive R&D activities to show, that on-spec, semi-synthetic multiblends can be produced from several different synthetic fuels. One important aspect is the emission of soot particles from aircraft engines. The Multiblend Jet A-1 has been analyzed in a flow reactor setup regarding the formation of soot precursor compounds in comparison to a reference Jet A-1. The experiment revealed a lower formation of relevant soot precursors which also corresponds to the higher hydrogen content of the Multiblend Jet A-1 compared to the reference fuel. The lower soot formation in a real aircraft engine has been proven during ground runs of an A300-600 aircraft with PW4158 engines. The Multiblend Jet A-1 showed lower particle number and particle mass emission than the reference fuel. The difference to the reference fuel decreased with increasing power settings. In summary, the emission of particle mass is reduced by ~29% and the number of emitted particles is reduced by ~37% if the ICAO landing-and-take-off cycle is used for evaluation.

Introduction

The aviation sector is facing particular challenges surrounding climate protection targets in light of the Paris Climate Agreement. Prior to the worldwide COVID-19 pandemic, the aviation industry showed growth rates between 3 % and 6 % (2015 – 2019) [1]. Despite the strong decrease in flight movements in 2020, the aviation industry will also require high amounts of jet fuel in the future. The use of sustainable aviation fuels (SAF) as a substitute for fossil fuels will play an important role in reducing CO_2 emissions in aviation and fulfilling future regulations on greenhouse gas emissions. A further driver for the increased application of alternative jet fuels is the increasing relevance of airports as an emission source of ultra-fine particles (UFP). Several studies worldwide showed the release of UFP into the environment that could be attributed to jet engine emissions [2-5]. Aircraft jet engines release volatile and non-volatile particles which feature different aerosol dynamics, airborne transport range and exposure potential [6, 7]. Lab and field studies with alternative jet fuel blends have demonstrated that jet fuels with an elevated hydrogen content (low amount of unsaturated hydrocarbons) show lower soot emissions than a regular reference Jet A-1 for the same engine [8-12]. However, in order to use SAF in aviation, compliance with sustainability criteria have to be monitored along the entire supply chain. Furthermore, it must be ensured that fuel mixtures containing different alternative fuel components do not deviate from current fuel specifications for Jet A-1 (“drop-in fuel”).

The primary goal of the research and demonstration project on the use of renewable kerosene at Leipzig/Halle Airport (short: DEMO-SPK) was to examine and verify the behavior of blends of several renewable SAF with fossil Jet A-1 under realistic conditions in the supply infrastructure of a major airport. Another aim was to successfully demonstrate the use of Multiblend Jet A-1 in the general fuel supply infrastructure, from procurement to aircraft fueling operations, on the international level for the first time. The key results are promising [13]. The project demonstrated that the supply chain for Multiblend Jet A-1 was technically feasible and that the fuel could be used without making any changes in normal operating procedures. The project also verified that the use of Multiblend Jet A-1 resulted in a reduction of about 35 % in

CO_2 equivalents compared with pure fossil Jet A-1. A number of solutions and recommendations to facilitate practical use were developed as well [13].

This study aims to summarize the findings with regard to the emission of ultra-fine particles from the use of the Multiblend Jet A-1 produced within the framework of DEMO-SPK. Two types of alternative jet fuel mixtures have been analyzed in a flow reactor experiment regarding their expected soot formation potential. Due to limitations in the availability of certain fuel components only one mixture has been tested on the engines of an A300 regarding the soot emission in comparison to a reference Jet A-1. In order to use multiblends, they have to comply with the fuel specification ASTM D7655 and have to possess sufficient storage stability. This has been evaluated prior to the campaign to avoid biases of the experiment. The results of this study demonstrate the positive impacts of SAF application in a real airport environment.

Materials and Methods

Fuels One reference Jet A-1 and two alternative jet fuel blends were tested on a lab-scale basis. Multiblend Jet A-1 was a ternary mixture of 30 %v/v HEFA (hydroprocessed esters and fatty acids) fuel, 8 %v/v ATJ (alcohol-to-jet) fuel and 62 %v/v reference Jet A-1. The second blend (Multiblend Jet A-1 + SIP) consisted of 17 %v/v HEFA, 3 %v/v ATJ, 75 %v/v Jet A-1 and 5 %v/v SIP (synthesized iso-paraffins). All fuels comply with the requirements of ASTM D7566-20b. The reference fuel used for blending and for the on-site emission test originated from the same refinery (Lingen) but not necessarily from the same batch. It should be noted that the Lingen refinery was selected for the DEMO-SPK project because of its stable properties across batches. The engine ground runs were performed with one of the alternative jet fuel blends (Multiblend Jet A-1) and the reference fuel (Reference Jet A-1). Minor changes in some fuel parameters can be expected due to residues in storage tanks, fuel trucks and piping (see Table SI1). Therefore, fuel samples were taken from the aircraft fuel tank after each ground run for analysis. The relevant parameters are summarized in Table 1 (see Supporting Information for test methods).

Fuel Characterization and Stability 900 L of Multiblend Jet A-1 + SIP and 400 L of Multiblend Jet A-1, respectively, were prepared and stored in tanks of the type TA 950 (Rietbergwerke GmbH & Co KG, material steel S355J2 with a hot-dip galvanized surface). The tanks were kept outdoors under a roof, exposed to the ambient climatic conditions during the storage period from April to October 2018 in Erding, Germany. However, they were protected from rain and sunlight. Samples were taken from both fuel blends at the beginning and at the end of the storage period and were subjected to a full analysis to determine possible alterations in fuel quality (see SI for test methods). The relevant fuel parameters are shown in Table 4.

Table 1: Selected physico-chemical parameters for the three different fuels of the lab-scale experiments (lab) and from the aircraft (A/C).

Parameter	**Reference Jet A-1**	**Multiblend Jet A-1**	**Multiblend Jet A-1 + SIP**	**ASTM D 7566 Requirement**
Components	Jet A-1	Jet A-1/ HEFA/ATJ	Jet A-1/HEFA/ ATJ/SIP	
Sample	A/C[a]	A/C[a]	Lab	
Aromatics [%v/v]	15.5	9.9	12.0	8–25
Density (15°C) [kg/m³]	808.8	787.2	797.9	775–840
Freezing point [°C]	-72.6	-58.2	-63.4	< -47
Flash point [°C]	42.0	42.0	48.0	> 38
Viscosity (-20°C) [mm²/s]	3.872	3.753	4.365	< 8
Viscosity (-40°C) [mm²/s]	7.302	7.099	8.753	< 12
Net Heat of Combustion [MJ/kg]	43.187	43.527	43.400	> 42.8
Smoke point [mm]	24.0	30.0	26.8	> 25.0
Naphthalenes [%v/v]	0.28	n.d.	0.18[b]	< 3.0
Sulfur, total [%m/m]	0.0027	0.0099	0.0018	< 0.30
Lubricity [mm]	0.65	0.68	0.62	< 0.85
Hydrogen content [%m/m]	13.72	14.30	n.d.	-
	13.788	14.319	14.138	
Distillation				
Initial boiling point [°C]	152.1	152.3	161.3	reported
10% vol. recovered [°C]	170.7	168.6	178.1	< 205
50% vol. recovered [°C]	193.7	192.2	202.3	reported
90% vol. recovered [°C]	225.9	231.4	233.0	reported
Final boiling point [°C]	257.8	256.0	248.6	< 300

[a]The fuel parameters were determined from a sample taken from the aircraft fuel tank after the ground run; [b]calculated; n.d.: not determined.

Lab-scale flow reactor measurement The oxidation of jet fuels was investigated at DLR's high-temperature flow reactor with coupled molecular-beam mass spectrometry (MBMS) to estimate the influence of the kerosene composition on the kinetic reaction process during

combustion. In previous studies detailed description of the atmospheric MBMS flow reactor system [14-16] as well as the signal evaluation [17-19] is given and only a brief summary is provided in the following.

The reactor setup consists of a ceramic flow tube (40 mm inner diameter, 1000 mm heated length) placed in a high-temperature oven with temperature-controlled gas inlet to avoid condensation effects of the pre-evaporated fuel. Detection takes place at the reactor outlet using a time-of-flight mass spectrometer (TOF-MS) with electron ionization (nominal electron energy of 13.5 eV). The in-situ gas sampling is carried out at ambient pressure (~980 mbar) with a handmade quartz nozzle (25° internal angle, 1-2 mm wall thickness, 80 mm total length). The extracted gas sample is expanded into a high vacuum and thus converted into a molecular beam. A nickel skimmer transfers the molecular beam into the ionization chamber where the neutral molecules are ionized. Species identification is performed on the basis of the exact mass (mass resolution R = 3000) [15].

The fuels' oxidation was performed under lean (Φ = 0.8) and slightly rich (Φ = 1.2) combustion conditions within a temperature range of 800 - 1200 K by applying a continuous decreasing temperature ramp (-200 K/h), starting with complete oxidation and ending with non-reactive state. Premixed gases are fed to the flow reactor highly diluted within the argon carrier gas (Ar > 99 %v/v), whereby a self-sustaining combustion reaction is suppressed. Reaction temperatures are known for any condition [19]. The liquid fuels were pre-evaporated before entering the reactor. Table 2 presents the specific gas flow rates for the respective fuels and oxidizer (O_2) at consistent argon flow (17.64 g/min). The fuels' hydrogen content was determined using pulsed nuclear magnetic resonance (NMR) according to ASTM D7171 (Table 1) to calculate the respective stoichiometry conditions. Heteroatoms were neglected. For both stoichiometry series a constant carbon flow was taken into account and the oxidizer amount was adjusted accordingly. The resulting differences in the total volume flow are negligible. The flow rates are controlled by mass flow controllers (Bronkhorst, Mini CORI-FLOW™) with high accuracy and repeatability.

Table 2: Gas flow rates [mg/min] for examined combustion conditions of the fuels' oxidation at consistent argon flow (17.64 g/min).

Fuel	Abbreviation	Fuel [mg/min]	Oxidizer O_2 [mg/min]	
		Φ=0.8 | Φ=1.2	Φ=0.8	Φ=1.2
Reference Jet A-1	Ref	31.08	131.7	87.8
Multiblend Jet A-1	MB	31.27	133.6	89.1
Multiblend Jet A-1 + SIP	MB SIP	31.20	133.0	88.7

Signal quantification is performed by use of cold-gas-mixtures ("direct") and via the empirical approximation method of relative ionization cross sections (RICS) after the signals were adjusted for background and fragmentation contributors. The uncertainty of the quantification reaches a maximum of 20 % if using direct calibration. In case of the RICS-method the uncertainty may increase by a factor of 2 to 4 [15] if ionization properties of the target species are unknown. It is important to note that signal contribution of isomers cannot be separated by use of electron ionization (EI) and therefore no differentiation of the molecular structure is possible. Assignment of chemical structure is solely based on experience gained by isomer-specific methods such as photoelectron photo ion coincidence spectroscopy (PEPICO) [19-21] that are typically applied to investigate combustion reactions of neat substances.

Engine emission measurement Two ground runs ("reference run" / "multiblend run") were performed with an A300-600 (freight version) equipped with two Pratt & Whitney PW4158 engines. The engine runs were performed in a noise protection hangar at Leipzig/Halle airport on the 30th September 2018. The air inlets of the hangar are designed to provide a laminar flow along the aircraft and the engines. Therefore, side-winds do not affect the measurement. The probe sampling was performed at the edge of the hangar at 2.5 m height and aligned to engine 1. The setup is visualized in the project video of DEMO-SPK [22] and the Supporting Information. The distance between sampling inlet and engine exhaust plane was 20 m. For each fuel, 7 different engine power settings were tested (see Table 3). The ambient temperature rose from 6 – 10°C (reference run) to 16°C (multiblend run) over the day. In case of the highest power setting (85 % N1), the relative uncertainty of the fuel flow is higher than in the other cases. This is caused from the manual operation of the thrust which led to a small

delay in reaching the target level and the shorter operating time. The time-resolved development of the parameters is illustrated in Figure SI2.

Table 3: Operation parameters and test matrix of the ground runs (in the order of execution).

			Reference run			Multiblend run		
ID	%N1[a]	t [min]	FF[b] [kg/h]	T25[c] [°C]	EGT[d] [°C]	FF[b] [kg/h]	T25[c] [°C]	EGT[d] [°C]
Start	23	8	699 ± 6	12.2 ± 0.2	354 ± 1	632 ± 6	20.5 ± 0.4	331 ± 4
1	40	8	1286 ± 11	22.5 ± 0.2	326 ± 1	1254 ± 24	31.3 ± 0.7	328 ± 9
2	60	5	2609 ± 15	45.6 ± 0.5	358 ± 1	2631 ± 15	55 ± 0.4	376 ± 1
3	50	8	1868 ± 11	33.4 ± 0.5	335 ± 1	1840 ± 10	41.6 ± 0.5	351 ± 1
4	30	8	880 ± 12	16.5 ± 0.5	335 ± 2	900 ± 20	24.7 ± 0.4	351 ± 2
5	85	1.5	6173 ± 370	88.1 ± 4.0	457 ± 11	6175 ± 16	99.1 ± 0.7	475 ± 2
Cool	23	8	691 ± 8	13.3 ± 0.9	366 ± 7	695 ± 6	20.5 ± 0.8	384 ± 12
6	75	5	4382 ± 27	71.6 ± 1.2	414 ± 2	4310 ± 12	78.9 ± 0.4	428 ± 1
7	23	8	690 ± 7	14.2 ± 0.5	364 ± 1	691 ± 6	20.7 ± 0.5	377 ± 1

[a]Fan speed of the low pressure turbine; [b]Engine fuel flow; [c]Inlet temperature of the high pressure turbine; [d]Exhaust gas temperature of the combustion chamber.

The sampled aerosol was transferred via a heated 45 m sampling line (ID = 5.6 mm, 120°C) to the measuring container. The undiluted aerosol was measured via an Engine Exhaust Particle Sizer (EEPS, TSI Inc.) equipped with a thermal denuder (300°C, Dekati Ltd.). The EEPS measures particles in the range between 5.6 nm and 560 nm in 32 channels at 10 Hz. Further measurements on the diluted aerosol were performed with a 3022A CPC (TSI Inc.), a MA-200 Aethalometer (AethLabs) and a Scanning Mobility Particle Sizer (SMPS, TSI Inc.). The MA-200 recorded the data in a 5 s interval. The SMPS consisted of a 3082 Classifier, a 3081 Long-DMA, 3088 Aerosol Neutralizer and a 3776 CPC. The SMPS measured a particle size distribution between 8 nm and 279 nm every 60 s. The aerosol was diluted with a DI-1000 diluter (Dekati Ltd.) by factor 20.7 ± 0.9. The inlet pressure of the diluter was kept stable at 950 mbar with a pressure controller (Burkert Fluid Control Systems). Nitrogen oxides were measured via chemiluminescence using a CLD700 (Ecophysics, undiluted) and a CLD64 (Ecophysics, diluted). The diluted carbon dioxide concentration was monitored with a LI-7200RS Enclosed Path CO_2/H_2O Analyzer (LI-COR). General combustion products (e.g. CO, NO_x, total hydrocarbons) were monitored with a MKS 2030 FT-IR instrument (undiluted). The full setup is summarized in Figure 1.

Data analysis The measured particle concentrations were converted into emission indices using the CO_2 concentration recorded by the LI-7200RS. The calculation follows the recommendation in AIR6241. The non-volatile particle number (nvPN) is derived from the data of the EEPS and the non-volatile particle mass (nvPM) is derived from the MA-200 aethalometer. Since the particle number concentration of the CPC could not be corrected for the particle loss in the sampling system, the data was used for orientation purposes only and are not presented in the manuscript. The OPS data is also not included in this manuscript due to the low number of particles with d > 300 nm. The results of the SMPS featured insufficient statistics in the present experiment which not allowed measuring the total number of emitted particles. Therefore, the SMPS was used for the loss correction analysis only.

Loss correction The loss of particles in the sampling system is a vital parameter that must be considered for jet engine emission experiments [23]. In the present case, the particle loss rate is determined experimentally using a portable aerosol generator. A sodium chloride test aerosol with a count mode diameter of 42 nm is introduced into the probe inlet and the concentration is recorded for 5 min by the SMPS. The procedure is repeated at the inlet of SMPS afterwards. The ratio between the inlet concentration and outlet concentration for each channel of the SMPS is calculated and the penetration curve is fitted from the obtained results (Figure 2). The test aerosol features a broad particle size distribution (PSD) which covers the range of the engine exhaust target aerosol. The experimental data from the SMPS and the EEPS have been corrected for particle losses using the fitted penetration curve function. The high particle loss is expected to be caused by the high residence time of ~10 s even though the flow in the sampling tube is laminar (Re = 997).

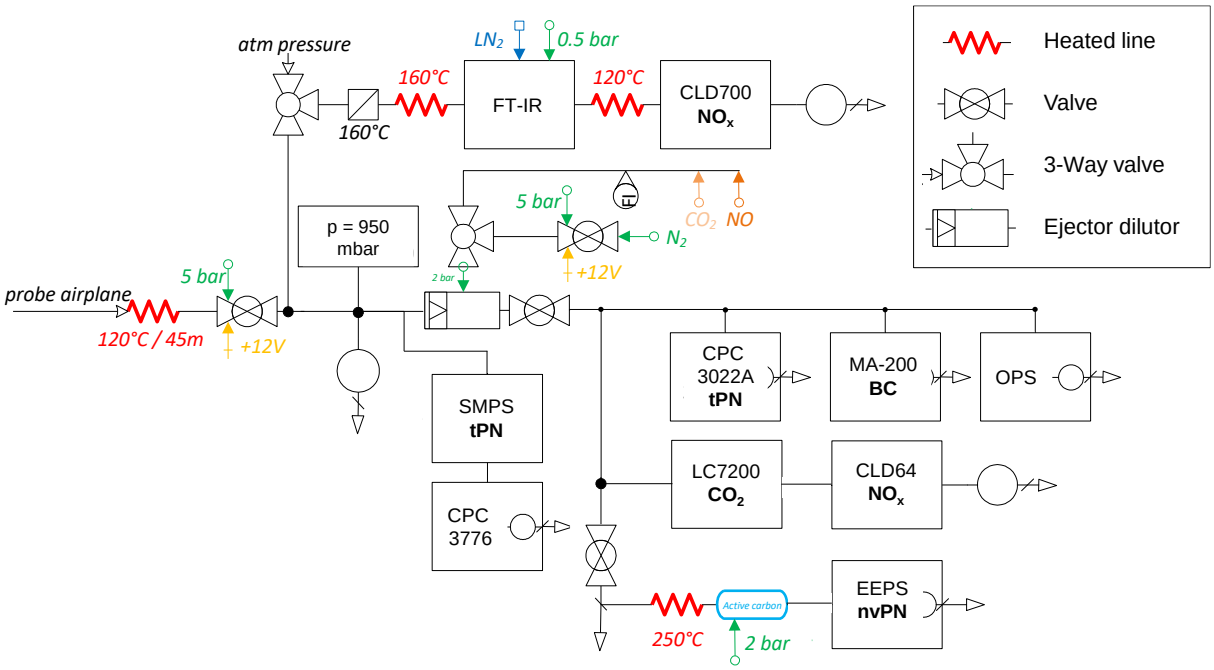

198

199 Figure 1: Experimental setup of the engine emission measurement

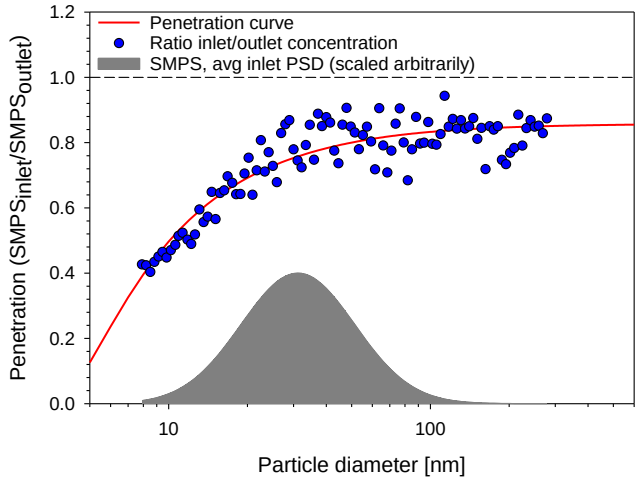

200

201 Figure 2: Experimental loss correction function of the sampling system based on the ratio
202 between the particle size distribution at inlet and outlet.

203

204 **Results and Discussion**

205 *Fuel Characterization and Stability*

206 Analysis results of Multiblend Jet A-1 and Multiblend Jet A-1 + SIP before and after storage
207 are summarized in Table 4. The analysis of both Multiblend mixtures confirmed that ASTM
208 D7566-compliant fuels had been obtained. This demonstrates that on-spec, semi-synthetic
209 fuel mixtures can readily be produced from several different synthetic fuels. The comparison

of physico-chemical parameters before and after storage shows only variations within the range of the uncertainty of the applied test methods. Therefore, no deterioration of fuel quality was found after the storage period.

Table 4: Physico-chemical parameters of two alternative jet fuel mixtures before and after storage

Parameter	**Multiblend Jet A-1 + SIP**		**Multiblend Jet A-1**		**Unit**	**ASTM D 7566 Requirement**
	Before storage	**After storage**	**Before storage**	**After storage**		
Acidity, total	0.002	0.002	0.002	0.002	mg KOH/g	< 0.10
Aromatics	12.0[a]		9.9[a]		%v/v	8–25
Distillation						
Initial Boiling Point	161.3	160.5	159.0	159.1	°C	reported
10 %v/v recovered (T10)	178.1	177.8	174.2	174.7	°C	< 205
50 %v/v recovered (T50)	202.3	202.6	198.8	199.0	°C	reported
T50–T10	24.2	24.8	24.6	24.3	°C	> 15
90 %v/v recovered (T90)	233.0	233.4	232.2	232.6	°C	reported
T90–T10	54.9	55.6	58.0	57.9	°C	> 40
Final Boiling Point	248.6	252.7	251.2	253.0	°C	< 300
Distillation residue	1.2	1.2	1.2	1.2	%v/v	< 1.5
Distillation loss	1.1	1.0	1.0	1.0	%v/v	< 1.5
Flash point	48.0	47.0	45.5	45.5	°C	> 38
Density at 15°C	797.9	798.0	789.0	789.0	kg/m³	775–840
Freezing point	-63.4	-63.4	-57.0	-57.0	°C	< -47
Lubricity	0.618	0.616	0.655	0.665	mm	< 0.85
Viscosity (−20°C)	4.365	4.355	4.198	4.112	mm²/s	< 8
Viscosity (−40°C)	8.753	8.862	8.142	8.149	mm²/s	< 12
Existent gum	<1	<1	1.2	<1	mg/100ml	< 7
Deposit rating	1	1	1	1	-	<3
Pres. Drop	0	0	0	0	mmHg	< 25
Net Heat of Combustion	43.400	43.400	43.525	43.527	MJ/kg	> 42.8
Corrosion copper strip	1a	1a	1a	1a	-	< 1
Smoke Point	26.8[b]	27.5[b]	28.7[b]	28.3[b]	mm	> 25.0
Naphthalenes	0.18		0.15		%v/v	< 3.0
Sulfur, total	0.0018	0.0019	0.0016	0.0016	%m/m	< 0.30

[a]aromatics and naphthalene content was calculated and is only given once; [b]<25.0 mm or >18.0 mm and Naphthalenes <3.0 %v/v

Flow Reactor Experiment

The flow reactor experiment provides a basis for the estimation and explanation of pollutant emission patterns, especially soot formation, in technical combustion systems. However, it should be noted that this data set reflects homogeneous gas phase reactions only and thus is focused on the chemical pollutant formation potential of the fuel. For technical combustion systems, like turbofan engines, the combustion reaction is accompanied by complex interactions of fuel atomization, fuel vaporization, fluid dynamics and the chemical reaction network. All of these sub-processes can influence the final pollutant emissions of the engine. Therefore, the combination of flow reactor measurements and full-scale engine experiments is useful to illustrate and explore the impact of alternative jet fuels on engine exhaust emissions.

Major species (stable products and oxidizer) for the three tested fuels are shown in Figure 3 as a function of the oven temperature. The temperature can be considered as an indicator of the reaction progress. At relatively cold oven temperatures, no reaction takes place and the reactants (kerosene and oxygen) pass through the reaction zone unchanged. Starting at a temperature of approx. 800 K, degradation of the fuel components begins, which is accompanied by moderate oxygen consumption and formation of first intermediates. With increasing temperature, carbon oxide and elemental hydrogen are formed. Chain-branching reactions lead to an exponential increase in the radical pool and thus to a rapid increase in reaction rate. This leads to significant oxygen consumption and carbon monoxide is oxidized to carbon dioxide. Subsequently, only reaction products can be detected at the reactor outlet beyond 1050 K. For lean condition (Φ = 0.8) CO_2, H_2O, and a corresponding excess of O_2 is present as product, while for slightly-rich conditions (Φ = 1.2) CO and H_2 are added as products. The major species profiles of the three investigated jet fuels are qualitatively and quantitatively very similar (same plot pattern) and are in line with previous findings for certified kerosene [16, 24, 25]. Thus, the ternary fuel blending with alternative kerosene does not lead to significant changes in the global reaction behavior under the examined conditions.

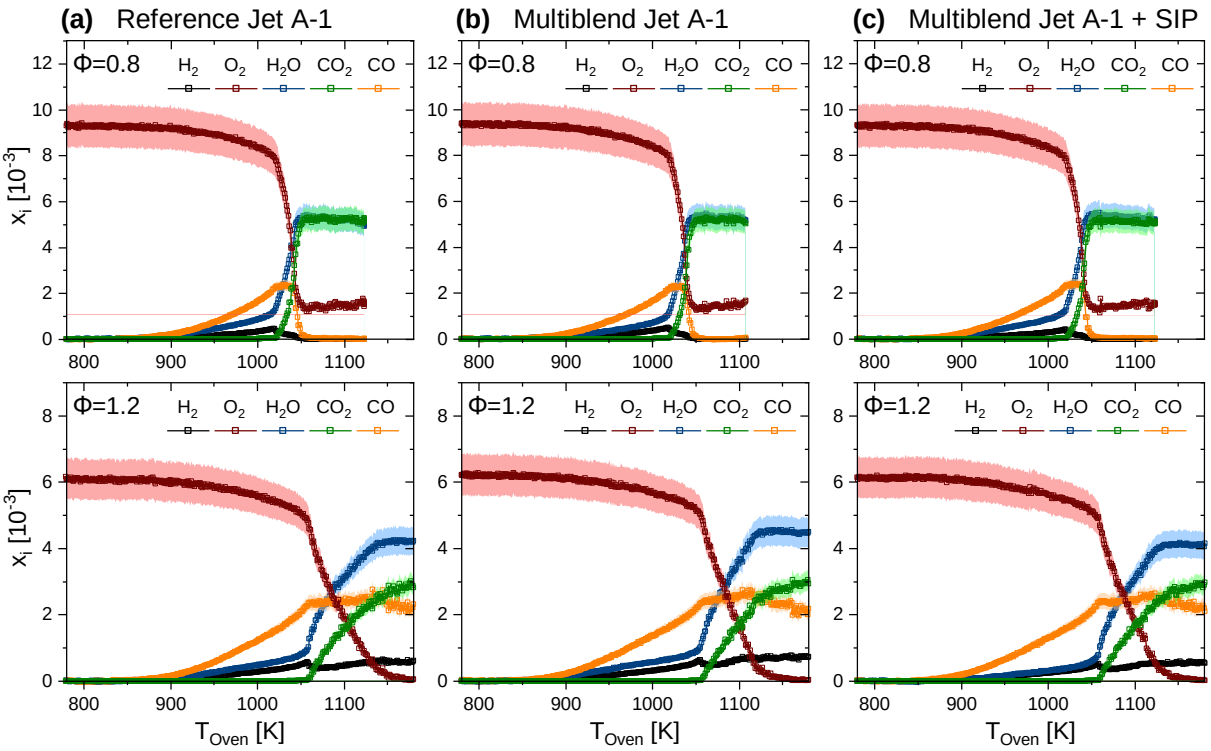

Figure 3: Mole fraction with uncertainty bars of major species (H_2, H_2O, O_2, CO_2, CO) from oxidation of the technical jet fuels under lean (Φ = 0.8) and slightly-rich (Φ = 1.2) conditions.

Figure 4 shows selected main stable intermediates, including small hydrocarbons (a), like methane (CH_4) and ethylene (C_2H_4) as well as formaldehyde (CH_2O) as representatives of carbonyl compounds (b) for slightly-rich conditions (Φ = 1.2). These species occur in combustion reactions of almost all hydrocarbons and their concentration shows only a slight dependence on the fuel composition. This is given in the inserts of Figure 4, where the fuels' hydrogen content is used to represent the molecular structure of the fuels. Due to higher proportion of aliphatic components, the alternative blends (MB and MB SIP) have higher hydrogen content than the fossil reference kerosene (Ref). For methane, no fuel dependency can be determined considering the experimental scatter. The ethylene concentration increases slightly with the addition of alternative components and higher hydrogen content of the fuels, respectively. This can be attributed to the methyl branching of the open-chain aliphatic compounds present in HEFA and SIP which tends to favor the formation of C3 fragments. A slight but detectable increase can also be observed for formaldehyde.

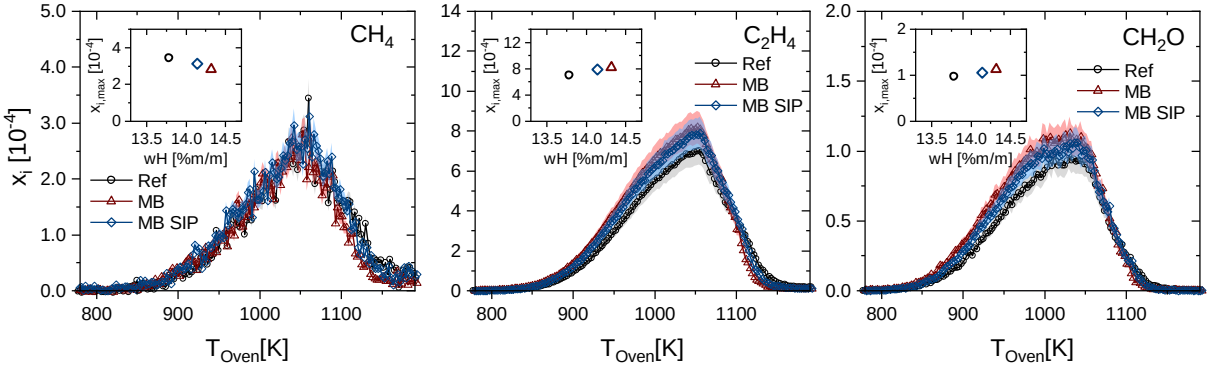

Figure 4: Mole fraction with uncertainty bars of selected small intermediates: Methane (CH_4), ethylene (C_2H_4), and formaldehyde (CH_2O) from the oxidation of the technical jet fuels under slightly-rich conditions (Φ = 1.2). Insert: Maximum mole fraction as a function of the fuels' hydrogen content (wH) [%m/m].

In contrast to the previous mentioned intermediates, the maximum mole fractions of aromatic soot precursors show a clear correlation with the hydrogen content of the kerosene. This is illustrated for slightly-rich (Φ = 1.2) combustion conditions in Figure 5. Here, the development of important soot precursor species, such as, benzene (C_6H_6), styrene (C_8H_8), indene (C_9H_8), naphthalene ($C_{10}H_8$), acenaphthylene ($C_{12}H_8$), and anthracene ($C_{14}H_{10}$) is summarized. The concentration of these soot precursors species decreases according to the following sequence: Reference Jet A-1 (Ref) > Multiblend Jet A-1 + SIP (MB SIP) > Multiblend Jet A-1 (MB). Beside the dependence on the fuel composition, a decrease in the concentrations with increasing molecule size of the soot precursors can be recorded in accordance with previous findings [25-27]. Thus, a reduction in the concentration of soot precursor species by about one third for oxidation of the multiblends compared to the fossil reference kerosene can be observed. For example, the reduction of benzene in the case of the Multiblend Jet A-1 is almost 33 % for both stoichiometries.

On the basis of the flow reactor experiment, a significant reduction of the soot emission can be expected in a real engine when changing from the reference kerosene to the Multiblend Jet A-1. It is very important to note that the observed reduction of the soot precursor species cannot be transferred into a real combustion system quantitatively. However, the trends in both parts of the experiment should be in alignment.

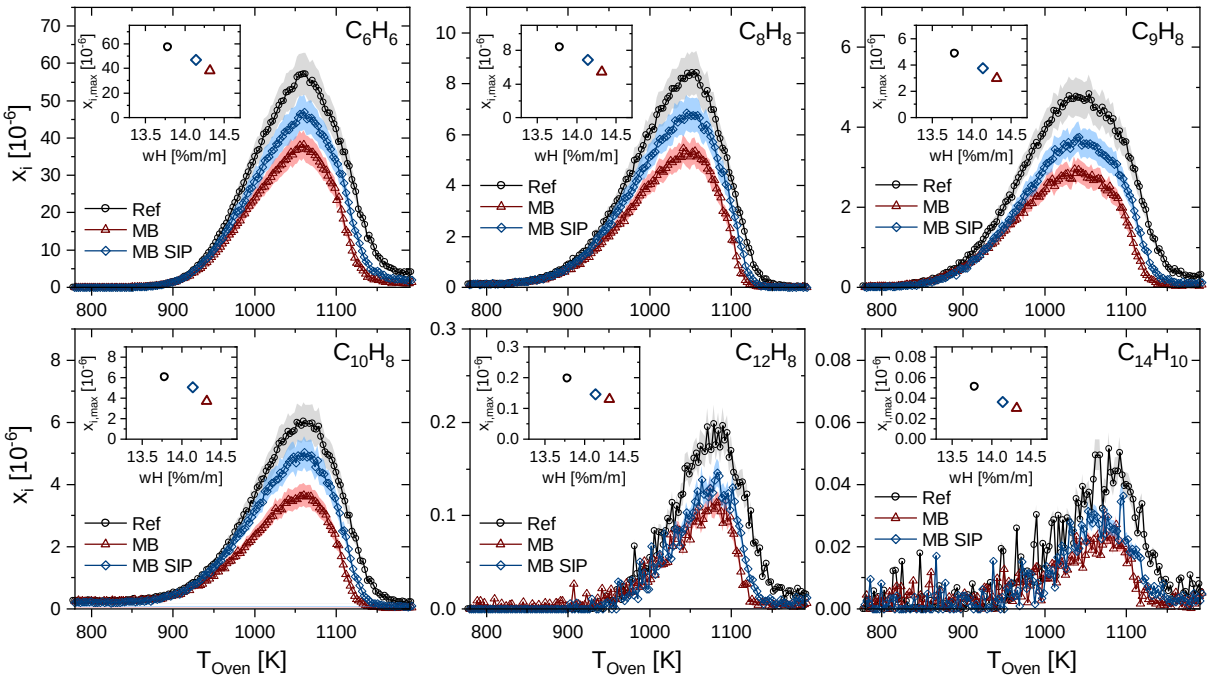

Figure 5: Mole fraction with uncertainty bars of selected soot precursors: benzene (C_6H_6), styrene (C_8H_8), indene (C_9H_8), naphthalene ($C_{10}H_8$), acenaphthylene ($C_{12}H_8$), and anthracene ($C_{14}H_{10}$) from the oxidation of the technical aviation fuels under rich conditions (Φ = 1.2). Insert: Maximum mole as a function of the fuels' hydrogen content (wH) [%m/m].

Jet Engine Experiment

As expected from the lab-scale experiment, the application of the alternative jet fuel blend led to a reduction in particle number emission and particle mass emission for all power settings in the full-scale engine experiment (Figure 6). The engine particle emission profile of the PW4158 engine showed a minimum at approx. 30 % - 40 % N1. In case of the non-volatile particle number emission index, the highest emission was observed for the lowest power setting. Published information on the particle emission characteristics of the PW4158 engine is limited. The ICAO database reports a smoke number of 8.1 for the highest power setting (T/O). Timko et al. [28] provide emission data for engine runs using a fuel with 600 ppm sulfur and 16.2 % aromatics. However, the reported particle emission indices (shown in Figure 6) are an average of several sampling distances (1, 15, 30, 43 and 50 m behind the engine). Therefore, additional uncertainties can be expected due to the evolution of the plume. The correlation between the results of the reference run and the published values is best for the highest and lowest power setting. Based on the aromatic content of the fuel, the values are expected to be between the reference Jet A-1 and the Multiblend Jet A-1. It must be noted, however, that the nvPM

emission correlates with fuel hydrogen content [29] which does not necessarily correlate with aromatic content [10]. Considering the fuel uncertainty and the different instruments used (PM: MA-200 / MAAP; PN: EEPS/CPC), the overall correlation is acceptable.

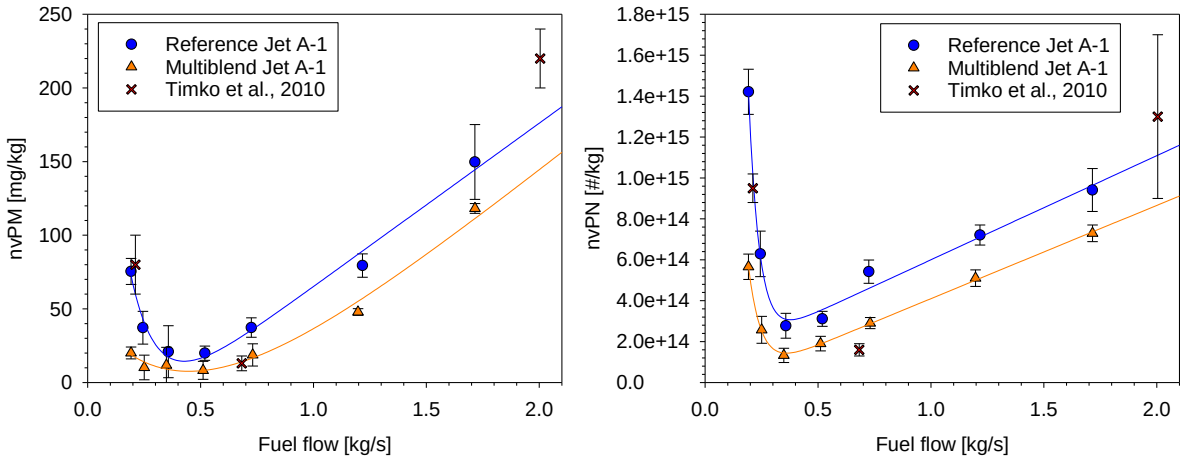

Figure 6: Particle mass emission index (left, MA-200) and particle number emission index (right, EEPS) for the reference fuel and the alternative jet fuel blend. Emission indices for the PW4158 engine from Timko et al. [28] are shown for comparison.

Regarding the size of the emitted particles no significant shift in the particle size distribution can be observed for the two different fuels (Figure 7) at the same power setting. The main fraction of non-volatile particles features diameters below 30 nm which is typical for turbofan engine aerosols [9, 30]. The highest count mode diameter is observed for the highest power setting tested in both cases. This may be attributed to the fact that the highest particle number concentration is observed for this setting and coagulation occurs in this slightly aged aerosol. Changing the fuel from the reference Jet A-1 to the Multiblend Jet A-1 had the highest impact on the lowest two power settings (23 % N1 and 30 % N1). The emission of particle mass is reduced by ~73 % and the emission of particle number is reduced by ~60 % for these cases (Figure 8). The effect decreases with increasing power setting. In order to evaluate the overall impact of the fuel change on the released amount of particles, the emission during the ICAO landing-and-take-off cycle (LTO) has been calculated on the basis of the measured engine emission profile (Figure 6). The measured power settings have been adjusted on the target power settings of the LTO cycle (7 % thrust for 26 min, 30 % thrust for 4 min, 85 % thrust for 2.2 min, 100 % thrust for 0.7 min) based on the fuel flow of the engine. In the present

experiment, the application of the Multiblend Jet A-1 led to a 37 % reduction in the released particle number and a 29 % reduction in released particle mass. It must be noted that the 100 % thrust setting has been extrapolated from the obtained data. Despite the correlation with published values (Figure 6) a large uncertainty may be expected for this power setting. However, the impact of this elevated uncertainty is insignificant considering the fact that only 9 % of the total reduction is caused from changes at the T/O power setting (Figure 8).

Considering the results of both experiments, the observed effect of soot reduction by using the alternative kerosene can be directly attributed to the chemical combustion reactions and therefore to the chemical composition of the multiblend itself. A beneficial effect of alternative fuel components, such as HEFA, ATJ, and SIP, on particulate emissions can be expected over a wide range of different combustion conditions. It is promising that the results from the actual full-scale gas turbine combustor is consistent with earlier fundamental work performed in the flow reactor and laminar diffusion flames. For instance, the observations are in line with Saffaripour et al. [31] who observed a significant reduction in soot emissions by investigation of laminar diffusion flames of Jet A-1 and different synthetic jet fuels based on Fischer-Tropsch processes. Furthermore, a correlation between the soot precursor species benzene and soot volume fractions on the centerline of the flame was stated. The qualitative trend is observed by several studies [8, 11, 24] in which an alternative Fischer-Tropsch-component has shown lower sooting propensity compared to conventional Jet A-1. A lower sooting tendency, represented by a higher Smoke Point (SP) for alternative jet fuel blends and their neat alternative components, like synthetic- and iso-paraffinic kerosene (SPK and IPK), HEFA, and ATJ compared to petroleum-derived kerosene (JP-8) was also determined by Won et al. [32].

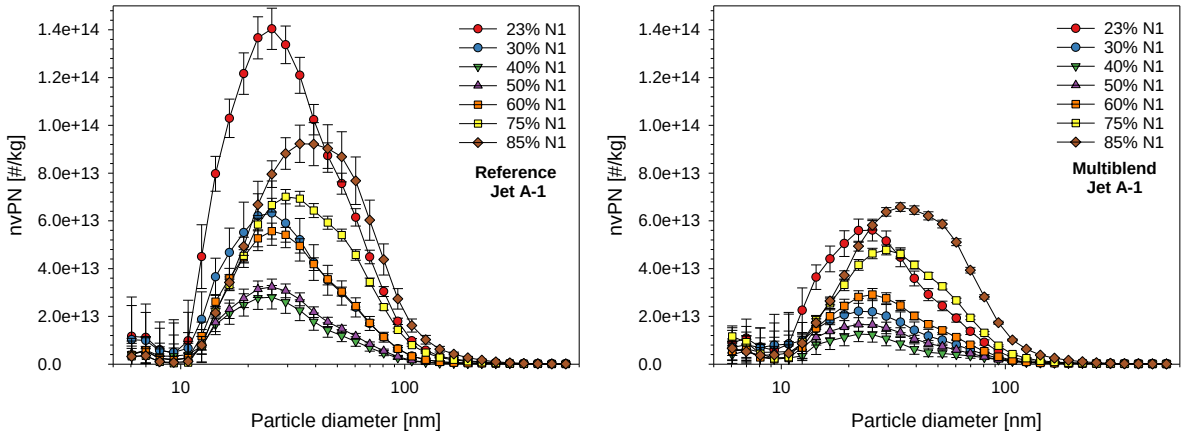

335

336 Figure 7: Non-volatile particle number size distribution (EEPS) for the engine ground runs with
337 reference Jet A-1 (left) and Multiblend Jet A-1 (right).

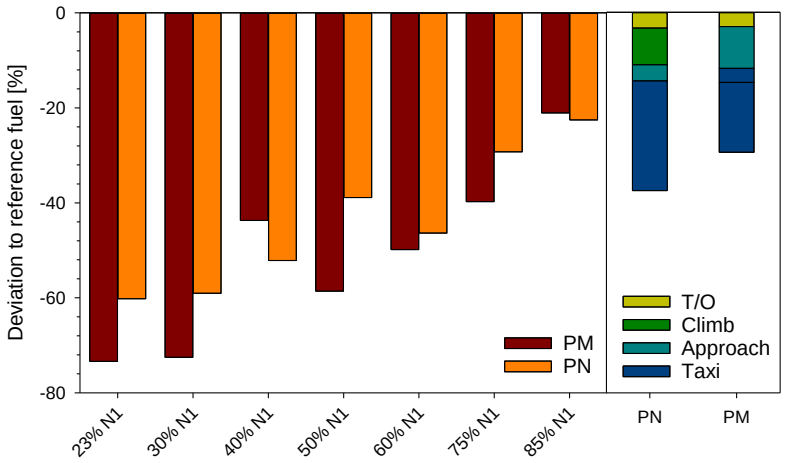

338

339 Figure 8: Particle number emission and particle mass emission reduction by the Multiblend Jet
340 A-1 compared to the reference fuel for the tested power settings (left) and for the LTO cycle
341 (right). The value for take-off (T/O) has been estimated from the interpolation in Figure 6.

342 **Conclusions**

343 The experiment demonstrated the successful application of a ternary alternative jet fuel
344 blending practice. On-spec, semi-synthetic fuel mixtures can be produced from several
345 different synthetic fuels and be stored over the period of 6 months without the deterioration of
346 fuel quality. The tendency to form soot from the different fuels was predicted in a flow reactor
347 experiment on lab-scale basis. The trend in soot emission, which follows the hydrogen content
348 of the fuels, could be demonstrated by engine runs at ground level. A change in other emission
349 parameters was not observed in this context and the development of intermediates showed no
350 significant deviation in the oxidation process. The emission of particle mass is reduced by ~29

% and the number of emitted particles is reduced by ~37 % if the ICAO landing-and-take-off cycle is used for evaluation. The experiment demonstrated the flexible use of alternative jet fuel components within the safety margins of the fuel specifications and their positive impact on the jet engine particle emission. Further investigations are necessary to provide a correlation between lab-scale experiments and real world engines to accelerate the development and optimization of alternative jet fuel blends with minimized particle emission.

Acknowledgements

The research and demonstration project on the use of renewable kerosene at Leipzig/Halle Airport (in short: DEMO-SPK) involved the collaboration of more than 20 international partners from industry and science. It was initiated as a model project of the Mobility and Fuel Strategy (MFS) and financed by the Federal Ministry of Transport and Digital Infrastructure (BMVI). In addition to thanks to the whole project team, the authors are especially grateful for the support and effort of European Air Transport Leipzig (EAT) and DHL which provided the A300 and made the ground run experiments possible. The authors especially thank Nico Tenius and Lars Remmers for their personal commitment to make this campaign successful.

References

[1] Berster P, Gelhausen M, Pabst H, Wilken D. DLR-Global Aviation Monitor March 2020 - Analysis and Short Term Outlook of Global, European and German Air Transport. Cologne: German Aerospace Center; 2020.

[2] Hudda N, Gould T, Hartin K, Larson TV, Fruin SA. Emissions from an International Airport Increase Particle Number Concentrations 4-fold at 10 km Downwind. Environmental Science & Technology 2014;48(12):6628-35, https://doi.org/10.1021/es5001566.

[3] Ren JL, Liu JJ, Li F, Cao XD, Ren SX, Xu B, et al. A study of ambient fine particles at Tianjin International Airport, China. Science of the Total Environment 2016;556:126-35, https://doi.org/10.1016/j.scitotenv.2016.02.186.

[4] Pirhadi M, Mousavi A, Sowlat MH, Janssen NAH, Cassee FR, Sioutas C. Relative contributions of a major international airport activities and other urban sources to the particle number concentrations (PNCs) at a nearby monitoring site. Environmental Pollution 2020;260:10, https://doi.org/10.1016/j.envpol.2020.114027.

[5] Stacey B, Harrison RM, Pope F. Evaluation of ultrafine particle concentrations and size distributions at London Heathrow Airport. Atmospheric Environment 2020;222:12, https://doi.org/10.1016/j.atmosenv.2019.117148.

[6] Yu ZH, Timko MT, Herndon SC, Richard CML, Beyersdorf AJ, Ziemba LD, et al. Mode-specific, semi-volatile chemical composition of particulate matter emissions from a commercial gas turbine aircraft engine. Atmospheric Environment 2019;218:8, https://doi.org/10.1016/j.atmosenv.2019.116974.

[7] He RW, Gerlofs-Nijland ME, Boere J, Fokkens P, Leseman D, Janssen NAH, et al. Comparative toxicity of ultrafine particles around a major airport in human bronchial epithelial (Calu-3) cell model at the air-liquid interface. Toxicol Vitro 2020;68:10, https://doi.org/10.1016/j.tiv.2020.104950.

[8] Lobo P, Condevaux J, Yu ZH, Kuhlmann J, Hagen DE, Miake-Lye RC, et al. Demonstration of a Regulatory Method for Aircraft Engine Nonvolatile PM Emissions Measurements with Conventional and Isoparaffinic Kerosene fuels. Energy & Fuels 2016;30(9):7770-7, https://doi.org/10.1021/acs.energyfuels.6b01581.

[9] Moore RH, Thornhill KL, Weinzierl B, Sauer D, D'Ascoli E, Kim J, et al. Biofuel blending reduces particle emissions from aircraft engines at cruise conditions. Nature 2017;543(7645):411-5, https://doi.org/10.1038/nature21420.

[10] Schripp T, Anderson B, Crosbie EC, Moore RH, Herrmann F, Osswald P, et al. Impact of Alternative Jet Fuels on Engine Exhaust Composition During the 2015 ECLIF Ground-Based Measurements Campaign. Environmental Science & Technology 2018;52(8):4969-78, https://doi.org/10.1021/acs.est.7b06244.

[11] Kinsey JS, Squier W, Timko M, Dong YJ, Logan R. Characterization of the Fine Particle Emissions from the Use of Two Fischer-Tropsch Fuels in a CFM56-2C1 Commercial Aircraft Engine. Energy & Fuels 2019;33(9):8821-34, https://doi.org/10.1021/acs.energyfuels.9b00780.

[12] Schripp T, Herrmann F, Oßwald P, Köhler M, Zschocke A, Weigelt D, et al. Particle emissions of two unblended alternative jet fuels in a full scale jet engine. Fuel 2019;256:115903, https://doi.org/10.1016/j.fuel.2019.115903.

[13] Müller-Langer F, Dögnitz N, Marquardt C, Zschocke A, Schripp T, Oehmichen K, et al. Multiblend JET A-1 in Practice: Results of an R&D Project on Synthetic Paraffinic Kerosenes. Chem Eng Technol 2020;43(8):1514-21, https://doi.org/10.1002/ceat.202000024.

[14] Köhler M, Osswald P, Xu HB, Kathrotia T, Hasse C, Riedel U. Speciation data for fuel-rich methane oxy-combustion and reforming under prototypical partial oxidation conditions. Chemical Engineering Science 2016;139:249-60, https://doi.org/10.1016/j.ces.2015.09.033.

[15] Oßwald P, Köhler M. An atmospheric pressure high-temperature laminar flow reactor for investigation of combustion and related gas phase reaction systems. Review of Scientific Instruments 2015;86(10):105-9, http://dx.doi.org/10.1063/1.4932608.

[16] Köhler M, Osswald P, Krüger D, Whitside R. Combustion Chemistry of Fuels: Quantitative Speciation Data Obtained from an Atmospheric High-temperature Flow Reactor with Coupled Molecular-beam Mass Spectrometer. J Vis Exp 2018(132):10, https://doi.org/10.3791/56965.

[17] Herrmann F, Jochim B, Osswald P, Cai LM, Pitsch H, Kohse-Höinghaus K. Experimental and numerical low-temperature oxidation study of ethanol and dimethyl ether. Combustion and Flame 2014;161(2):384-97, https://doi.org/10.1016/j.combustflame.2013.09.014.

[18] Herrmann F, Osswald P, Kohse-Höinghaus K. Mass spectrometric investigation of the low-temperature dimethyl ether oxidation in an atmospheric pressure laminar flow reactor. Proceedings of the Combustion Institute 2013;34:771-8, https://doi.org/10.1016/j.proci.2012.06.136.

[19] Osswald P, Hemberger P, Bierkandt T, Akyildiz E, Köhler M, Bodi A, et al. In situ flame chemistry tracing by imaging photoelectron photoion coincidence spectroscopy. Review of Scientific Instruments 2014;85(2):11, https://doi.org/10.1063/1.4861175.

[20] Bierkandt T, Hemberger P, Osswald P, Krüger D, Köhler M, Kasper T. Flame structure of laminar premixed anisole flames investigated by photoionization mass spectrometry and photoelectron spectroscopy. Proceedings of the Combustion Institute 2019;37(2):1579-87, https://doi.org/10.1016/j.proci.2018.07.037.

[21] Krüger D, Osswald P, Köhler M, Hemberger P, Bierkandt T, Karakaya Y, et al. Hydrogen abstraction ratios: A systematic iPEPICO spectroscopic investigation in laminar flames. Combustion and Flame 2018;191:343-52, https://doi.org/10.1016/j.combustflame.2017.12.025.

[22] BMVI. Erneuerbares Kerosin: Forschungs- und Demonstrationsvorhaben (DEMO-SPK) Flughafen Leipzig/Halle; 2019. Available from: https://www.youtube.com/watch?v=Fj--omcYeVc.
[23] Durand EF, Crayford AP, Johnson M. Experimental validation of thermophoretic and bend nanoparticle loss for a regulatory prescribed aircraft nvPM sampling system. Aerosol Science and Technology:15, https://doi.org/10.1080/02786826.2020.1756212.
[24] Jürgens S, Osswald P, Selinsek M, Piermartini P, Schwab J, Pfeifer P, et al. Assessment of combustion properties of non-hydroprocessed Fischer-Tropsch fuels for aviation. Fuel Process Technol 2019;193:232-43, https://doi.org/10.1016/j.fuproc.2019.05.015.
[25] Oßwald P, Whitside R, Schäffer J, Köhler M. An experimental flow reactor study of the combustion kinetics of terpenoid jet fuel compounds: Farnesane, p-menthane and p-cymene. Fuel 2017;187:43-50, https://doi.org/10.1016/j.fuel.2016.09.035.
[26] Chu TC, Buras ZJ, Oßwald P, Liu MJ, Goldman MJ, Green WH. Modeling of aromatics formation in fuel-rich methane oxy-combustion with an automatically generated pressure-dependent mechanism. Physical Chemistry Chemical Physics 2019;21(2):813-32, https://doi.org/10.1039/c8cp06097e.
[27] Kathrotia T, Oßwald P, Köhler M, Slavinskaya N, Riedel U. Experimental and mechanistic investigation of benzene formation during atmospheric pressure flow reactor oxidation of n-hexane, n-nonane, and n-dodecane below 1200 K. Combustion and Flame 2018;194:426-38, https://doi.org/10.1016/j.combustflame.2018.05.027.
[28] Timko MT, Onasch TB, Northway MJ, Jayne JT, Canagaratna MR, Herndon SC, et al. Gas Turbine Engine Emissions-Part II: Chemical Properties of Particulate Matter. J Eng Gas Turbines Power-Trans ASME 2010;132(6):15, https://doi.org/10.1115/1.4000132.
[29] Moore RH, Shook M, Beyersdorf A, Corr C, Herndon S, Knighton WB, et al. Influence of Jet Fuel Composition on Aircraft Engine Emissions: A Synthesis of Aerosol Emissions Data from the NASA APEX, AAFEX, and ACCESS Missions. Energy & Fuels 2015;29(4):2591-600, https://doi.org/10.1021/ef502618w.
[30] Lobo P, Christie S, Khandelwal B, Blakey SG, Raper DW. Evaluation of Non-volatile Particulate Matter Emission Characteristics of an Aircraft Auxiliary Power Unit with Varying Alternative Jet Fuel Blend Ratios. Energy & Fuels 2015;29(11):7705-11, https://doi.org/10.1021/acs.energyfuels.5b01758.
[31] Saffaripour M, Zabeti P, Kholghy M, Thomson MJ. An Experimental Comparison of the Sooting Behavior of Synthetic Jet Fuels. Energy & Fuels 2011;25(12):5584-93, https://doi.org/10.1021/ef201219v.
[32] Won SH, Veloo PS, Dooley S, Santner J, Haas FM, Ju YG, et al. Predicting the global combustion behaviors of petroleum-derived and alternative jet fuels by simple fuel property measurements. Fuel 2016;168:34-46, https://doi.org/10.1016/j.fuel.2015.11.026.